Changes in Neuronal Signaling and Cell Stress Response Pathways are Associated with a Multigenic Response of *Drosophila melanogaster* to DDT Selection

Keon Mook Seong[1,*], Brad S. Coates[2], Weilin Sun[1], John M. Clark[3], and Barry R. Pittendrigh[1]

[1]Department of Entomology, Michigan State University, East Lansing, Michigan, USA

[2]Corn Insects & Crop Genetics Research Unit, USDA-ARS, Iowa State University, Ames, Iowa, USA

[3]Department of Veterinary & Animal Science, University of Massachusetts, Amherst, Massachusetts, USA

*Corresponding author: E-mail: seongkeo@msu.edu.

Accepted: November 30, 2017

Data deposition: The data sets generated during this study are available in the NCBI Sequence Read Archive (SRA) under accession numbers SRX2611754–SRX2611759 (https://www.ncbi.nlm.nih.gov/sra/; last accessed December 06, 2017).

Abstract

The adaptation of insect populations to insecticidal control is a continual threat to human health and sustainable agricultural practices, but many complex genomic mechanisms involved in this adaption remain poorly understood. This study applied a systems approach to investigate the interconnections between structural and functional variance in response to dichlorodiphenyltrichloroethane (DDT) within the *Drosophila melanogaster* strain *91-R*. Directional selection in 6 selective sweeps coincided with constitutive gene expression differences in DDT resistant flies, including the most highly upregulated transcript, *Unc-115 b*, which plays a central role in axon guidance, and the most highly downregulated transcript, the angiopoietin-like *CG31832*, which is involved in directing vascular branching and dendrite outgrowth but likely may be under *trans*-regulatory control. Direct functions and protein–protein interactions mediated by differentially expressed transcripts control changes in cell migration, signal transduction, and gene regulatory cascades that impact the nervous system. Although changes to cellular stress response pathways involve 8 different cytochrome P450s, stress response, and apoptosis is controlled by a multifacetted regulatory mechanism. These data demonstrate that DDT selection in *91-R* may have resulted in genome-wide adaptations that impacts genetic and signal transduction pathways that converge to modify stress response, cell survival, and neurological functions. This study implicates the involvement of a multigenic mechanism in the adaptation to a chemical insecticide, which impact interconnected regulatory cascades. We propose that DDT selection within *91-R* might act systemically, wherein pathway interactions function to reinforce the epistatic effects of individual adaptive changes on an additive or nonadditive basis.

Key words: genome-wide evolution, fruit fly, insecticide resistance.

Introduction

Although adaptation by insect species to survive increasing exposures to insecticidal compounds poses a widespread threat to agriculture and human health (Mallet 1989; Ranson and Lissenden 2016), the systemic or genome-wide impacts of such adaptation are yet not fully understood. The classic paradigm ascribes arthropod resistance to insecticidal neurotoxicants either to the effects of one or perhaps several genes that facilitate the metabolic breakdown of xenobiotic compounds (Ffrench-Constant et al. 2004) or to modification of receptor proteins that inhibit toxin binding and their subsequent neurogenic effects (Ffrench-Constant et al. 1993; Ffrench-Constant 2013).

Indeed, low- to moderate-levels of DDT resistance in *Drosophila melanogaster* have been associated with single locus mutations in the sodium channel gene, *para* (Pittendrigh et al. 1997; Martin et al. 2000) in laboratory generated *para* mutant populations, as well as with metabolic resistance conferred by the upregulation of cytochrome P450s (Brandt et al. 2002; Daborn et al. 2007). In contrast,

high levels of DDT resistance in the *D. melanogaster* strain *91-R* is associated with multiple changes in physiology (Strycharz et al. 2013), with expression levels of ABC transporters (Strycharz et al. 2013; Seong et al. 2016), and with genes involved in xenobiotic detoxification, ion transport, transcription, and signal transduction (Pedra et al. 2004; Qiu et al. 2013). The necessity of candidate ABC transporters and P450s for DDT detoxification in stress response were functionally validated subsequently via RNAi knockdown (Gellatly et al. 2015); similarly, expression of several detoxification enzymes are controlled by the Nrf2/Keap2 pathway (Misra et al. 2013).

In general, many complex traits result from selection at multiple independent genetic loci (Najarro et al. 2015), and this likely extends to high levels of DDT resistance in *91-R* as well. Previously, structural signatures of adaptation to DDT within the genome of *91-R* were shown by near allelic fixation in 13 different genomic regions (Steele et al. 2015), with protein coding regions under the influence of directional selection (Steele et al. 2014). Specifically, the effects of DDT selection on 13 genome intervals on chromosomes 2L, 2R, and 3R in *91-R* were inferred by reductions in nucleotide diversity and corresponding estimates of directional selection using Tajima's *D* when compared with the susceptible control *91-C*. Additional functional analysis of the ABC transporter, MDR49, within a selective sweep of the *91-R* genome suggested a likely role in conferring DDT resistance (Seong et al. 2016). Despite these advances, the impact of these structural changes on functional variation between the *91-R* and its corresponding DDT-susceptible strain *91-C* remain not fully understood, particularly with respect to their relative contributions to DDT resistance levels.

The control of cell survival and the response to stress conditions involves intertwined sensing and response pathways, which include both general (constitutive) and stimulus-specific (inducible) interactions to modulate gene expression (Spriggs et al. 2010) leading to changes in cytoskeletal reorganization (Galbraith et al. 1998; Tzima et al. 2002), the accumulation of stress response proteins (Guertin et al. 2010), and changes within signal transduction pathways (Gehart et al. 2010). These responses often converge to effectively increase resilience to oxidative stress (Wang et al. 2003), regulate cell homeostasis (Slack et al. 2010), maintain the integrity of cellular DNA, lipids, and proteins via molecular chaperones (Tower 2011), and repair enzymes that help to increase fly lifespan (Shaposhnikov et al. 2015). For example, changes in pathways that modulate the expression of genes involved in detoxification and increased lifespan, such as the nuclear hormone receptor (NHR) insulin/insulin-like growth factor-like (IGF) signaling (IIS) pathway, may increase the capacity of an organism to resist cytotoxic effects of xenobiotics (Slack et al. 2011). Where the downstream IIS target the forkhead box-containing protein subfamily O, *FOXO*, transcription factors modulate the expression of genes involved in cycle control, metabolism, apoptosis, and cellular stress responses (Slack et al. 2011). More recently, the *Drosophila* NHR, DHR96, was shown to be a crucial factor for increasing resistance to DDT; while often co-occurring with IIS in natural conditions, it is functionally independent of IIS (Afschar et al. 2016). Thus, a multitude of metabolic responses and fixed adaptive mutations have been shown to contribute to DDT resistance in *91-R*, but the complex epistatic interactions and modifications to inclusive pathway components in relation to adaptations to xenobiotic resistance remain unknown. Moreover, DDT target site mutations and changes in neurologic function have not been discovered to date in *91-R*.

To partially address this knowledge gap, this study applied a systems approach to concurrently assess genome-wide structural and functional variation in the DDT resistant *D. melanogaster* strain *91-R*. Specifically, constitutive alteration of RNA-seq estimated transcript levels in *91-R* compared with its corresponding DDT-susceptible *91-C* counterpart were assessed in the context of regulatory pathways and any causal adaptive mutations underlying these changes.

Materials and Methods

Topical DDT Bioassay

To confirm resistance in *91-R*, we used a previously described bioassay approach with some modifications (Strycharz et al. 2013). Females (1–5 days old, mated) were used as the experimental group to assess adult mortality in *91-R* and *91-C* using an endpoint measure within a DDT topical application bioassay. Mortality rates were then analyzed within strain by the probit analysis (XLSTAT 2008, Addinsoft). The 50% lethal dose (LD_{50}), 95% confidence intervals, and slopes and intercepts for dose-response curves were generated.

RNA-Seq and Estimation of Differential Gene Expression

The DDT resistant *D. melanogaster* strain, *91-R*, and corresponding non-DDT selected control strain, *91-C*, were established previously (Merrell and Underhill 1956; Merrell 1960, 1965) and reared in separate colonies on a commercially available medium (Jazz-Mix Drosophila Food, Fischer Scientific) at 25 °C in plastic bottles with transfer to new bottles about every 2 weeks. The *91-R* strain has been continually selected by maintaining the flies in a colony bottle with the presence of a 150-mg DDT/filter paper disk while *91-C* was maintained without any exposure to DDT. A total of 1,000 5-day-old *D. melanogaster* flies (500 male and 500 female), not exposed to DDT within that generation, were pooled for each of three biological replicates per strain. Total RNA was extracted from each pool ($n = 6$) using the Qiagen RNeasy Maxi Kit according to the manufacturer's instructions (Qiagen, Valencia, CA). Bidirectional Illumina RNA-seq libraries were constructed from each pool, and 160-bp paired-end (PE) sequence read data generated on an Illumina HiSeq 2500 at the University of

Illinois Urbana-Champaign, W. M. Keck Center for Comparative and Functional Genomics (one lane per library; three lanes run for each *91-R* and *91-C* library). Six sequence runs were submitted to the National Center for Biotechnology Information (NCBI) sequence read archive (SRA; accession numbers SRX2611754-SRX2611759). Raw PE fastq-formatted read data were imported into the CLC Genomics Workbench software version 8.5 (Qiagen), each then individually trimmed to remove Illumina adapter sequences, low Phred quality regions ($q < 20$), short reads (<50 bp), and long oligo Ts (>50). The *Drosophila melanogaster* Release 6 reference genome assembly including annotated genes and transcripts was downloaded from Flybase database (http://flybase.org; last accessed December 06, 2017) (Dos Santos et al. 2015) and imported into the CLC Genomics Workbench RNA-seq Analysis Tool where trimmed RNA-seq read data from each library were independently aligned with parameters: minimum length fraction 0.9, minimum similarity fraction 0.8, insertion/deletion cost 3, and mismatch cost 3. Counts for the number of reads that aligned to each gene model were output in tab-delimited format.

Differences in gene expression (transcript abundance) were compared between *91-R* and *91-C* strains using the number of reads per kilobase per million (RPKM) of RNA-seq reads mapped against the annotated gene models in the *Drosophila* genome assembly v.6.07. Output was $\log_2$ transformed and normalized using the median method (Allison et al. 2006). Statistical significance of any differences in normalized read counts (expression levels) between strains were conducted using the "Exact Test" between two groups within the Differential Gene Expression tool of CLC Genomic Workbench (Robinson and Smyth 2008), as implemented in the EdgeR Bioconductor package (Robinson et al. 2010) to iteratively model dispersion for each gene used as a weighted average for subsequent comparisons (Robinson and Smyth 2007). Significances of any differences in RNA-seq reads mapped to gene models between *91-C* and *91-R* were corrected through multiple testing (Benjamini and Hochberg 1995). A low-stringency significance threshold of a corrected $\leq$0.01 FDR (false discovery rate) and $\log_2$ (fold change) $\geq|1.0|$, and a high-stringency threshold of a corrected $\leq$0.001 FDR and $\log_2$ (fold change) $\geq|2.0|$, were implemented when determining differential transcript expression.

Gene Expression by Reverse Transcriptase-Quantitative PCR

Reverse transcriptase-quantitative PCR (RT-qPCR) was carried out on selected transcripts for validation of RNA-seq estimated differences between the *91-R* and *91-C* strains. Both the RT-qPCR method and first-strand cDNA synthesis were similar to that previously described by Sun et al. (2015). Potential genomic DNA contamination was removed by treatment with RNase-free DNase (Qiagen). Relative expression was calculated using the $2^{-\Delta\Delta Ct}$ method (Livak and Schmittgen 2001) with *rp49* as the reference gene (Ponton et al. 2011). Multiple linear regressions were carried out using XLSTAT (Addinsoft) to compare relative expression based on RT-qPCR and RNA-seq for each gene.

To analyze differential gene expression at various developmental stages of the *91-R* and *91-C* strain, total RNA samples were prepared using RNeasy Mini Kit (Qiagen) from a pool of 20 eggs, an individual larva, an individual pupa, and an individual virgin adult female. At least three independent biological samples were prepared for each. The specific primer pairs for RT-qPCR were used (supplementary table S1, Supplementary Material online) with statistical analysis by XLSTAT (Addinsoft) using a two-way ANOVA followed by Tukey's multiple comparison tests for significant differences ($P < 0.05$) in gene expression during developmental stages.

Genome Positioning of Differentially Expressed Transcripts

Thirteen regions in the genome of *91-R* were previously defined as having undergone a selective sweep that reduced nucleotide diversities following DDT selection for survival (Selective sweeps 1–13; Steele et al. 2015). The genome intervals spanned by genes encoding differentially expressed transcripts were retrieved from Flybase.org and compare with the set of 100,000-bp intervals corresponding to the 13 selective sweeps. The gene symbols for differentially expressed genes (DEGs) within selective sweeps were used to query the collection of curated transcription factor (TF)-gene interactions maintained in the REDFly database (http://redfly.ccr.buffalo.edu; last accessed December 06, 2017) and experimentally supported TF-binding domain retrieved from modENCODE (http://www.modencode.org/; last accessed December 06, 2017). Corresponding upstream regulatory regions within extended gene regions were obtained from FlyBase.org, to which genomic read data were mapped and SNPs detected as described previously (Steele et al. 2014).

Ontologies, Pathways, and Interactions among Differentially Expressed Genes

For all transcripts surpassing the high-stringency threshold, information regarding protein–protein interaction from yeast-two-hybrid data were obtained from Flymine.org (Gene -> Interactions) and defined as first-order protein–protein interactions. Gene descriptions and protein domain information were retrieved from Flybase database (http://flybase.org; last accessed December 06, 2017) and Gene Ontology (GO) terms were retrieved from Flymine database (http://flymine.org; last accessed December 06, 2017) (Gene -> GO term queries). Additionally, the Flymine database (http://flymine.org; last accessed December 06, 2017) of phenotypes resulting from RNAi knockdown experiments (Gene -> RNAi phenotypes) were retrieved and clustered based on shared phenotypic term. The biochemical pathway

identifiers in which gene products reside were analogously obtained from Flymine.org (Gene -> pathway) and clustered by shared pathway. Functional interaction evidence (text mining, experimental, database, and coexpression data) was obtained from string-db version 10 (http://version10.string-db.org/; last accessed December 06, 2017) (Szklarczyk et al. 2015) for all derived gene products that surpassed the high-stringency threshold.

All of the above searches were analogously performed as well for yeast-2-hybrid partners for each DEG identified from interaction data (http://flymine.org/; last accessed December 06, 2017); Gene -> Interactions). Relevant pathway descriptions and pathways diagrams were obtained from the Kyoto Encyclopedia of Genes and Genomes (KEGG) database (http://www.genome.jp/kegg/pathway.html; last accessed December 06, 2017) Interactions among GO terms and RNAi phenotypes shared among yeast-2-hybrid partners for DEGs were visualized using Cytoscape 3.4.0 (Shannon et al. 2003), defining GO or RNAi phenotypes as the Target, DEG, and the Source, and yeast-2-hybrid partners as the Interaction. Regulation of each DEG (up- or down-) was used as a Source Attribute and mapped onto resulting networks.

Results

Topical DDT Bioassay

Mortalities among *91-R* adults after topical exposures of DDT were significantly lower compared with *91-C* when measured at a 24-h bioassay end-point. Specifically, the estimated LD_{50} values across replicates of *91-R* had a mean of 3,746.8 ng (2,577.2–5,202.2 ng, 95% CL) per individual versus 35.0 ng (31.9–38.4 ng, 95% CL) per individual for *91-C*, and a resultant >107.1-fold resistance to DDT among *91-R* compared with *91-C* (supplementary table S2, Supplementary Material online).

RNA-Seq and Estimation of Differential Gene Expression

Overall, ≥82.68% RNA-seq read data from replicates of *91-R* ($n = 3$) and *91-C* ($n = 3$; supplementary table S3, Supplementary Material online), from which 14,112,989 (8.9%) of the reads were trimmed, were subsequently aligned to the *D. melanogaster* genome v.6.07. Estimates of differential expression based on the normalized counts of RNA-seq read data that mapped to gene models predicted a total of 137 differentially expressed transcripts at the low-stringency, with 79 up- and 58 downregulated in *91-R* compared with *91-C* (supplementary table S4, Supplementary Material online) and; 69 transcripts for the high-stringency, with 42 up- and 27 downregulated (tables 1 and 2, respectively). Estimates of fold-change between 11 transcripts from *91-R* and *91-C* were highly correlated in the RT-qPCR and RNA-seq methods ($R^2 = 0.88$, $F = 102.2$, $P < 0.001$; supplementary fig. S1, Supplementary Material online).

Table 1
Annotations for Upregulated Transcripts in the DDT Resistant Strain *91-R*

Gene Symbol	Functional Annotation	Log_2 Fold Change[a]	FDR[b]
Unc-115b	Uncoordinated 115b	5.89	3.31E-06
Cyp4p2	Cytochrome P450-4p2	5.64	5.03E-04
Cyp6a8	Cytochrome P450-6a8	5.59	7.72E-92
Cyp4p1	Cytochrome P450-4p1	5.02	1.19E-27
Cyp6g1	Cytochrome P450-6g1	4.08	1.14E-23
Cyp6w1	Cytochrome P450-6w1	3.56	6.73E-94
Cyp6g2	Cytochrome P450-6g2	2.33	7.06E-03
CG14820	Peptidase_M14	3.82	7.05E-07
Qtzl	Quetzalcoatl	3.71	2.21E-04
CG7542	Trypsin	3.65	7.89E-45
CG31683	Unknown	3.58	4.30E-18
CG4250	Zn finger protein	3.54	6.20E-45
Jon65Aii	Jonah 65Aii	3.53	6.75E-23
Jon99Ci	Jonah 99Cii	2.28	1.10E-09
CG18787	Nucleoporin-like protein 2	3.52	1.23E-07
Mal-B1	Maltase-B1	3.44	7.64E-03
CG13658	Alpha-amylase	3.28	2.37E-06
CG5770	Peptidase_C11	3.04	3.71E-06
CG3819	Endonuclease_NS	2.96	4.55E-09
Npc2e	Niemann-Pick type C-2e	2.93	6.73E-03
CG33301	EcKinase	2.91	4.48E-17
CG43055	C-lectin domains-containing	2.86	1.61E-09
CG31703	RNA polymerase-associated protein RTF1	2.74	3.03E-03
Spn43Aa	Serpin 43Aa	2.73	6.17E-03
CG4210	Histone N-acetyltransferases	2.54	1.60E-04
Sfp24Ba	Seminal fluid protein 24Ba	2.50	1.76E-14
CG6908	EcKinase	2.20	1.99E-20
Lectin-galC1	Galactose-specific C-type lectin	2.16	5.23E-15
Sodh-2	Sorbitol dehydrogenase-2	2.14	2.85E-03
CG31809	Alcohol dehydrogenase	2.06	1.18E-04
CR33319	Unknown	4.84	2.16E-19
CR42653	Unknown	4.72	5.03E-04
CR44030	Unknown	4.65	1.80E-03
CR44308	Unknown	4.64	1.25E-04
CG33966	Unknown	4.34	1.80E-03
CG42521	Unknown	4.18	3.72E-05
CG31683	Unknown	3.58	4.30E-18
CR45191	Unknown	3.24	2.30E-04
CG14191	Unknown	3.23	3.91E-03
CR43239	Unknown	2.74	6.08E-07
CG6834	Unknown	2.71	7.23E-05
CG15293	Unknown	2.35	3.64E-66
CG33666	Unknown	2.25	2.98E-05

[a]Fold change was calculated as log2 *91-C/91-R*.
[b]FDR: False discovery rate. Differentially expressed genes were identified at the high-stringency threshold [FDR < 0.001 and log_2(fold change) ≥|2.0|] of *91-C/91-R*.

Stage-Specific Changes in Gene Expression

RT-qPCR measurements of a subset of transcripts differentially expressed across *91-R* and *91-C* egg, larva, pupa, and adult stages indicated that changes are mostly constitutive across those growth stages. Results showed that uncoordinated

Table 2

Annotations for Downregulated Transcripts in the DDT Resistant Strain *91-R*

Gene	Functional Annotation	Log_2 Fold Change[a]	FDR[b]
CG31832	Tyrosine kinase activator and a negative regulator of apoptosis	−6.76	7.33E-14
Ser12	Serine protease 12	−6.62	7.87E-09
CG30025	Serine protease	−5.13	2.79E-13
Hsp70Ba	Heat shock protein 70	−5.11	8.93E-03
PPO1	Prophenoloxidase 1	−4.35	1.17E-07
CG17234	Serine protease	−4.48	1.87E-03
CG31274	Leucine-rich_repeat	−3.57	1.23E-07
CG4927	Serine protease	−3.47	4.33E-03
CG30054	Guanine nucleotide-binding protein G(q) subunit alpha	−3.42	1.31E-05
PPO2	Prophenoloxidase 2	−3.31	1.87E-07
Hsp70Bb	Heat shock protein 70Bb	−3.28	8.56E-03
Jon99Fii	Jonah 99Fii	−3.24	1.05E-91
Cyp4e3	Cytochrome P450-4e3	−3.19	6.72E-18
CG3397	Aldo/keto reductaseNADP-dependent oxidoreductase	−3.06	2.93E-08
TotA	Turandot A	−2.83	1.44E-30
CG4563	AMP-dependent synthetase/ligase	−2.67	9.26E-04
CG2064	Alcohol dehydrogenase	−2.58	5.74E-12
CG31091	Abhydro lipase	−2.36	4.29E-04
TotC	Turandot C	−2.33	4.17E-11
CG43061	Pathogenesis	−2.31	4.58E-06
Idgf1	Imaginal disc growth factor 1	−2.26	7.47E-07
CG4757	Acetylcholinesterase	−2.19	7.78E-08
GILT2	Gamma interferon inducible lysosomal thiol reductase 2	−2.10	7.83E-33
CG6277	Lipase	−2.05	1.19E-11
CR33487	Unknown	−5.51	1.18E-05
CR43263	Unknown	−5.31	6.28E-03
CR43158	Unknown	−5.16	6.24E-06

[a]Fold change was calculated as log2 *91-C*/*91-R*.

[b]FDR: False discovery rate. Differentially expressed genes were identified at the high-stringency threshold [FDR < 0.001 and $\log_2$(fold change) $\geq |2.0|$] of *91-C*/*91-R*.

115b (*Unc-115b*) and jonah (*Jon*) 65Aii were constitutively more highly expressed in *91-R* compared with *91-C* across all stages (fig. 1), whereas imaginal disc growth factor 1 (*Idgf1*) was not differentially regulated in any stage (fig. 2). Several transcripts showed greater stage specificity. For example, the C-type lectin domain-encoding *CG43055* was predominantly expressed in the adult stage for both strains, but *91-R* had a ~15-fold higher level compared with *91-C*. In contrast, expression of the other C-type lectin, *Lectin-galC1*, occurred during larval and pupal stages (fig. 1). Similarly, *Jon99Cii* was predominantly expressed in the *91-R* larval and adult stages (fig. 1).

Interestingly, the serine protease inhibitor, *Spn43Aa*, was expressed predominantly in the pupal stage for both strains, but at ~4.02-fold higher levels in adults from *91-R* compared with *91-C* (fig. 1). Analogously, while *Jon99Fii* was highly expressed in larval stage for both strains, the transcript was ~1.9-fold more abundant in *91-R* larvae (fig. 2). Conversely, while the prophenoloxidases, *PPO1* and *PPO2*, were predominantly expressed during the larval stage for both strains, *91-C* showed a ~1.6- and ~2.25-fold higher expression as compared with *91-R* (fig. 2). In addition, changes in differential regulation between growth stages were shown for maltase-B1 (*MalB1*), with a higher expression during the pupal stage for *91-C* compared with *91-R* (fig. 1). Lastly, while of approximately equal expression level for *91-R* and *91-C* adults alike, the niemann-pick type C-2e (*Npc2e*) peptidoglycan recognition protein was the only transcript that partially conflicted with RNA-seq. In contrast, *Npc2e* was most highly expressed in *91-C* at the larval and pupal stages. Only *Unc-115b*, *Jon65Aii*, and *Idgf1* were expressed at high levels in eggs.

Genome Positioning of Differentially Expressed Transcripts

About 6 of the 69 DEGs based on RNA-seq analyses were colocated with genome regions of *91-R* previously placed within selective sweeps (e.g., reduced nucleotide variation; Steele et al. 2015). Four of these transcripts were upregulated in *91-R*, including the most highly upregulated transcript, *Unc-115b*, located within sweep 13 on chromosome 3R (table 3). The three remaining upregulated transcripts, *CG31683*, *CR43239*, and *Lectin-galC1*, resided within a successive series of regions with reduced nucleotide diversity along 2L. Two transcripts with reduced relative expression in *91-R*, *CR43263*, and *PPO2*, were colocated with selective sweeps on 2L (sweep 1) and 2R (sweep 11), respectively. This is based on a question if the 6 DEGs located within 178,075 bp (size of the 13 selective sweeps; Steele et al. 2014; $P = 3.369 \times 10^{-5}$) is more rare of an event as compared with 69 total DEGs being randomly distributed across the 143.9 Mb of the entire genome (4.795×10^{-7}). To do this, we calculated the *Z*-score for two population proportions, which provides *Z*-score of 0.0441 and a nonsignificant *P* value of 0.48405.

Promoters of 6 differentially expressed genes have 36 previously identified TF-gene interactions involving 25 different TFs (droidb.org database Feb 2017; 1.57 ± 0.79 promoters per TF). Four of these TFs, chromato (Chro), centrosomal protein 190kD (Cp190), CTCF, and trithorax (trx), all bind at upregulated *CG31683*, *Lectin-galC*, and *Unc-115b* (supplementary table S5, Supplementary Material online). Protein–protein interactions between boundary element-associated factor of 32kD (BEAF-32), Chro, and Cp190 are supported by yeast-2-hybrid experiments reported at Flybase.org (not shown). Furthermore, these four TFs, along with senseless (sens) and BEAF-32, bind the promoters of both *Unc-115b* and its nearest paralog, *Unc-115ba* (supplementary table S5, Supplementary Material online). The promoter binding domains in modENCODE provide evidence that these TFs are mostly positioned upstream of *Unc-115b* splice variants, except for variant *Unc-115b-RE* (fig. 3).

Mapping of pooled genomic-seq reads (Steele et al. 2014) identified three mutation sites that were within CHiP-seq

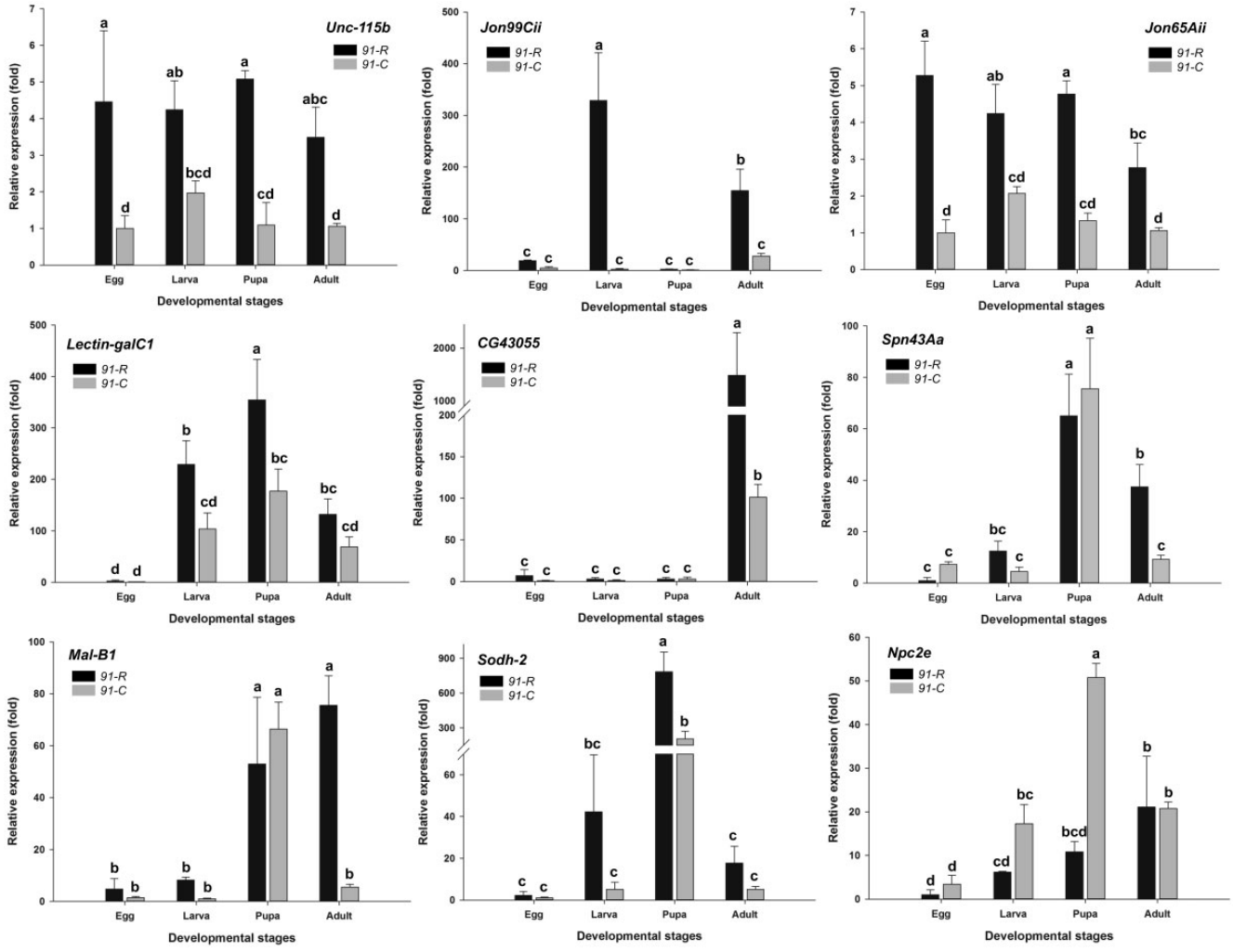

Fig. 1.—Relative expression levels of several upregulated genes in different developmental stages of *91-R* and *91-C strains* at the high-stringency threshold [FDR < 0.001 and $\log_2$(fold change) $\geq$|2.0|], determined by RT-qPCR. The mRNA level in different developmental stages was normalized using *rp49* as a reference gene. The mean expression in each developmental stage is shown as a fold change compared with the lowest mean expression, which has been ascribed an arbitrary value of 1. The vertical bars indicate standard error of the mean (SEM) ($n = 3$). Different letters on the bars indicate that the means are significantly different throughout the different developmental stages.

defined TF binding regions, and these mutations were also in or flanking consensus TF binding domains upstream of *Unc-115 b*. Specifically, the cAMP responsive element binding protein 1 (CRE-BP1) consensus binding sequence contained an indel (CTC insertion) and a substitution mutation within different reads from *91-R*. None of these mutations were present among reads from *91-C*. Additionally, a substitution mutation flanking a BEAF-32 recognition sequence (CGATA) was at higher frequency in *91-R* (0.60) compared with *91-C* (0.08).

Ontologies, Pathways, and Interactions among Differentially Expressed Genes

A total of 230 terms for molecular function (F; $n = 97$; 40 up- and 57 downregulated), biological process (P; $n = 92$; 59 up- and 33 downregulated), and cellular component categories (C; $n = 41$; 22 up- and 19 downregulated; supplementary fig. S2, Supplementary Material online) were assigned to DEGs. GO category C revealed extracellular region/space was highly represented among gene products from both up- and downregulated DEGs, and the GO category P showed oxidative–reductive processes were most prevalent among upregulated transcripts. GO category F showed heme and iron binding, as well as electron carrier activity, were most represented among upregulated transcripts, whereas serine-type endopeptidase activity was prevalent among downregulated transcripts (supplementary table S6, Supplementary Material online).

Reduction–oxidation (redox) activity was predicted among six upregulated cytochrome P450 monooxygenases (P450s; GO: 0016705) and sorbitol dehydrogenase 2 (*sodh-2*; GO:

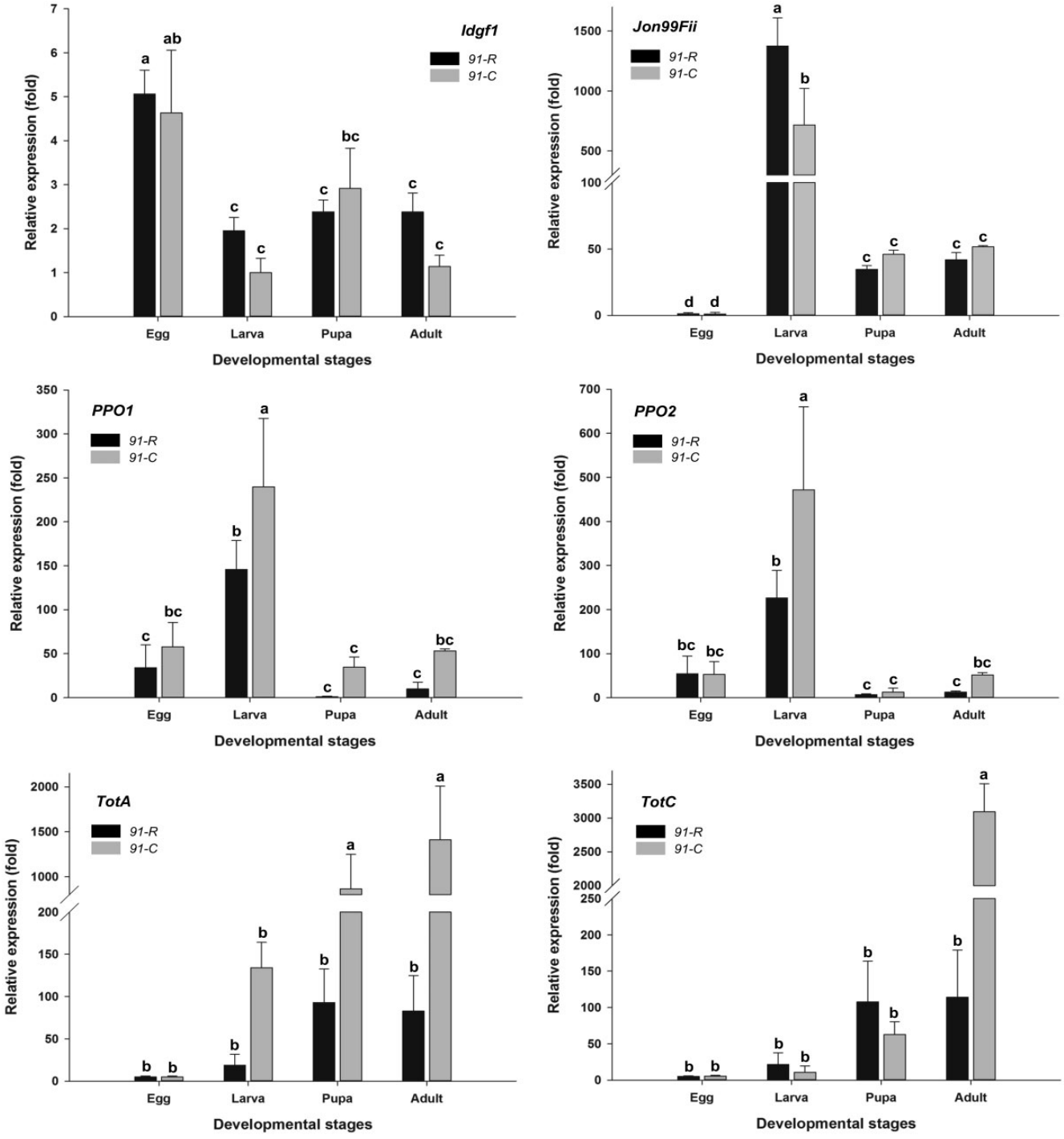

Fig. 2.—Relative expression levels of several downregulated genes in different developmental stages of *91-R* and *91-C strain* at the high-stringency threshold [FDR < 0.001 and $\log_2$(fold change) $\geq |2.0|$], determined by RT-qPCR. The mRNA level in different developmental stages was normalized using *rp49* as a reference gene. The mean expression in each developmental stage is shown as a fold change compared with the lowest mean expression, which has been ascribed an arbitrary value of 1. The vertical bars indicate standard error of the mean (SEM) ($n = 3$). Different letters on the bars indicate that the means are significantly different throughout the different development stages.

0055114) and analogously among downregulated gamma-interferon-inducible lysosomal thiol reductase 2, *GILT2*, and *PPO 1* and *2*. The second-most highly downregulated gene, serine protease 12 (*Ser12*), is annotated as an extracellular serine-like protease (GO: 0004185) involved in proteolysis (GO: 0006508) and wound healing (GO: 0042060).

Table 3

Differentially Expressed Transcripts Encoded within *91-R* Genome Regions Putatively under the Influence of Selective Sweeps in Response to DDT Selection

Gene	Functional Annotation	Log_2 Fold Change[a]	FDR[b]	Genome Position	Selective Sweep ID[c]
Unc-115b	Cytoskeletal linker protein that acts in axon guidance	5.89	3.31E-06	3R: 9,687,060–9,692,775	13
CG31683	Lipid metabolic process	3.58	4.30E-18	2L: 20,447,734–20,449,964	6
CR43239	Unknown	2.74	6.08E-07	2L: 17,353,730–17,354,668	4
Lectin-galC1	Immune pathway	2.16	5.23E-15	2L: 19,417,447–19,418,274	5
CR43263	Unknown	−5.31	0.006	2L: 1,216,854–1,217,785	1
PPO2	Immune pathway	−3.31	1.87E-07	2R: 9,042,261–9,044,709	11

[a]Fold change was calculated as log2 *91-C*/*91-R*.

[b]FDR: False discovery rate. Differentially expressed genes were identified on the basis of FDR < 0.001.

[c]Thirteen genomic intervals in *Drosophila melanogaster* strain *91-R* identified regions under the influence of a selective sweep (ID 1–13), where regions show reduced nucleotide diversity in *91-R* compared with *91-C* and putatively under the influence of directional selection in response to differential survivorship when exposed to DDT (Steele et al. 2015).

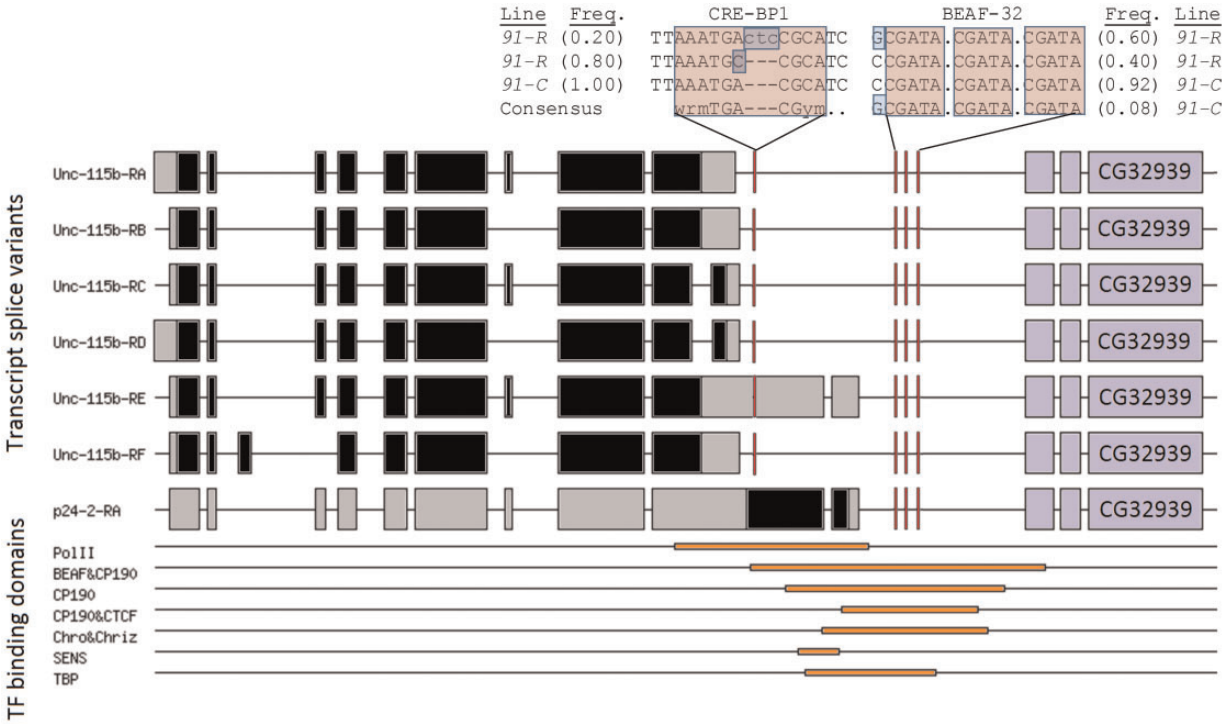

Fig. 3.—Splice variants for uncoordinated-115b (*unc-115b*; reverse strand of 3R) and corresponding putative upstream transcription factor binding domains; cAMP responsive element binding protein 2 (CRE-BP1), DNA polymerase II (DNA Pol II), TATA binding protein (TBP), BEAF-32 (boundary element-associated factor-32 kDa), CP190 (centrosomal protein 190 kDa), CTCF, Chro (Chromator), Chriz, and Sens (senseless). Flanking CG32939 defines the putative gene boundary.

Downregulated transcripts encoding serine proteases (GO: 0004252) include *CG17234*, *CG30025*, *CG4927*, and *Jon99Fii*. Of these, *CG17234* is involved in sensory perception of pain (GO: 0019233).

In addition to downregulated *PPO1* and *2*, turandot A and C (*TotA* and *TotC*), heat shock proteins (*Hsp70a* and *Hsp70b*), and *CG43061* respond to cellular stress or pathogen attack. Furthermore, DEGs may be involved in binding to actin (*Unc-115b*), myosin (*CG6834*), galactose (*Lectin-galC1* and *CG43055*), and lipids (*CG31683* and *Npc2e*). The most highly upregulated transcript, *Unc-115b*, has actin-binding function (GO: 0003779) and involvement in cytoskeletal organization (GO: 0007010). The most highly downregulated transcript, *CG31832*, is predicted to function as a transmembrane tyrosine kinase receptor (GO: 0030297) that negatively regulates apoptosis (GO: 0043066).

About 6 (14.3%) and 5 (11.9%) of 42 upregulated transcripts in *91-R*, respectively, encode cytochrome P450s and serine protease/serine protease-inhibitor-like domains (supplementary table S7, Supplementary Material online). Protein kinase domains are present in *CG6908*, *CG13658*, *CG6834*, and *CG33301*; *lectin C-type* domains were predicted in

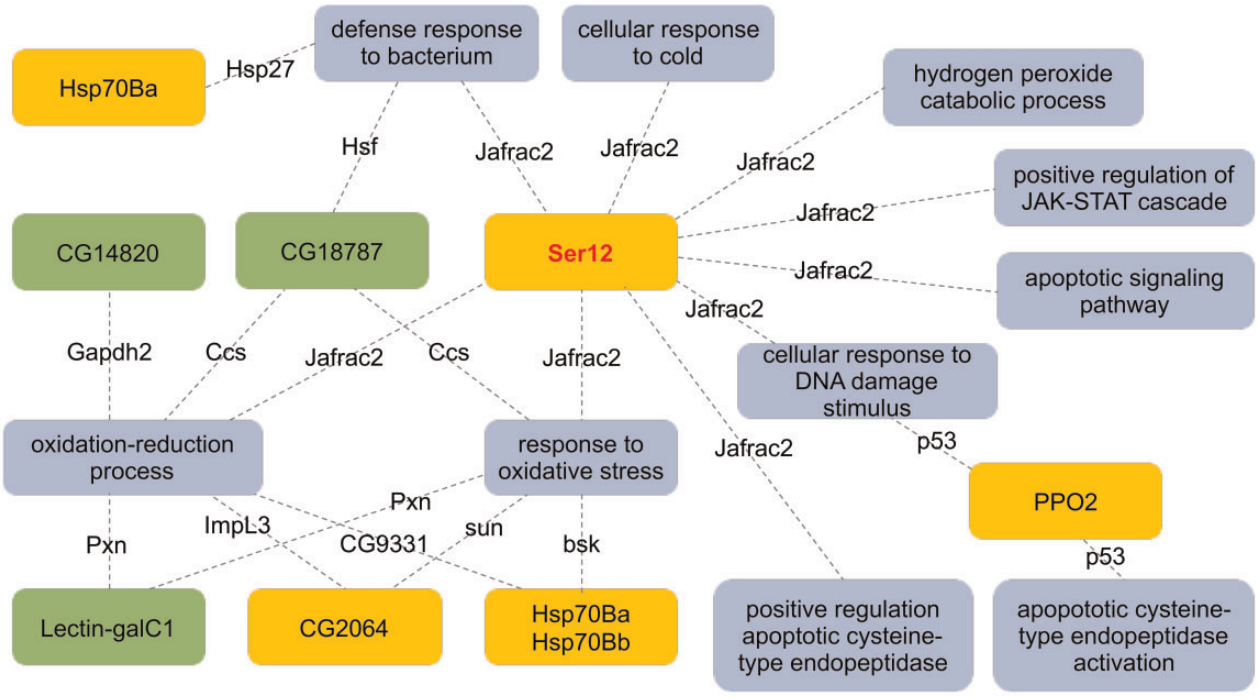

Fig. 4.—Functional interaction network connecting the downregulated serine protease, *Ser12*, to cellular pathways involved in apoptosis and response to stress. Protein–protein interaction and activation of the thioredoxin peroxidase 2, *Jafrac2*, by *Ser12* directly signals the activation of apoptotic cysteine-type endopeptidase, as well as potential regulatory cascades involving prophenol oxidase 2 (*PPO2*). *Jafrac2* is also involved in cellular response to oxidative stress conditions, and regulated cell survival via the Janus activated kinase/signal transducer and activator of transcription (JAK/STAT) pathway. Up- and down-regulated transcripts were indicated in green and orange boxes, respectively. Putative networks defined between DEGs and gene ontologies (biological processes; gray nodes) were connected by DEG yeast-2-hybrid protein–protein interaction partners.

derived protein products for *Lectin-galC1* and *CG43055*. The most highly upregulated *Unc-115 b* transcript predicts abLIM-type and villin headpiece domains.

Among the 34 pathways assigned to 19 of the 69 DEGs, 4—21.1%, the downregulated *Jon99Fii* and upregulated *Jon99Ci*, *Jon65Aii*, and *CG7542*—are involved in the activation of extracellular matrix metalloproteinases (MMPs; supplementary table S8, Supplementary Material online). All other pathways were represented by $\leq$2 protein coding genes. Five transcripts are nonprotein coding and received no GO or pathway annotations. Three protein coding genes (*CG14191*, *CG33666*, and *CR45191*) are of unknown function.

Protein–protein interactions derived from prior two-hybrid screens within Flymine identified 254 experimental lines of evidence for 201 unique interactions involving 33 DEGs (supplementary table S9, Supplementary Material online). High connectivity was shown via network analyses between downregulated *PPO1* and *PPO2* and upregulated *CG14820* through four different interactions, with *CG14820* interacting with the phosphatidylinositol-4-phosphate 5 kinase (*PIP5K*), skittles (*sktl*; supplementary fig. S3, Supplementary Material online). The downregulated *Hsp70Ba* and *Hsp70Bb* share 22 partners including the Jun N-terminal kinase (*bsk*). Additionally, the most highly upregulated transcript in *91-R*, *Unc-115 b*, physically interacts with the DNA mismatch repair proteins, *Mlh1* and *Pms2*, and the tetratricopeptide repeat domain-containing *Pex5*.

While no known interactions have been reported for the most highly downregulated transcript, *CG31832*, the second most highly downregulated *Ser12* interacts with thioredoxin peroxidase 2 (*Jafrac2*), with yeast-2-hybrid partner interactions showing an abundance of GOs related to stress response and control of apoptosis (fig. 4). Analogously, 8 up- and 6 downregulated transcripts (20.3% of DEGs) have protein network interactions that functionally impact neuron development or function (supplementary fig. S4, Supplementary Material online). Protein–protein interactions for 12 of 69 DEGs (17.4%) tether them to the cytoskeleton or extracellular matrix (supplementary fig. S5, Supplementary Material online).

Flymine Gene ->RNAi experiments identified 143 and 1,338 previously defined phenotypes, respectively, associations with the knockdown of 40 DEGs and 160 of their 205 yeast-2-hybrid partners (supplementary table S10, Supplementary Material online). Among the DEGs and partners, 44 (30.8%) and 354 (26.5%), respectively, were lethal (supplementary fig. S6, Supplementary Material online).

Among the remaining phenotypes associated with DEGs, changes in the phosphorylation state of extracellular signal-regulated kinase (*ERK*) was most prevalent ($n = 12$ phenotypes) following knockdown of nine different transcripts (*CG4250*, *CG4563*, *CG4927*, *CG7542*, *Cyp4e3*, *Hsp70Ba*, *Idgf1*, *Mal-B1*, and *Ser12*). This was followed by 11 RNAi phenotypes that resulted in alteration of wing development and flight capacity through the knockdown of *CG5770*, *CG6277*, *CG6834*, *Cyp6g1*, *CG6908*, *CG14191*, and *CG18787*. In addition, bristle morphology or development was impacted in eight different cases when seven different transcripts were knocked down (*CG14191*, *CG4757*, *CG5770*, *CG6277*, *CG6834*, *Sodh-2*, and *TotA*). Other phenotypes involved changes in Ca^{2+} transport and altered pathogen defenses, heat avoidance behaviors, and neural defects.

Discussion

In this study, we identified constitutive differentially expressed genes in DDT resistant *91-R* that are associated with neural cell development, signal transduction, and gene regulatory cascades that impact the nervous system. Previously, significant differences in expression were documented for several cytochrome P450s (*Cyp6a2*, *Cyp6g1*, and *Cyp9c1*) between DDT resistant *91-R* and the susceptible strain *Canton-S* (Qiu et al. 2013), as well as *Cyp6g1* between *91-R* and *Wisconsin* strain (Pedra et al. 2004). Moreover, use of UAS-RNAi transgenic lines of *D. melanogaster* has validated the role of several cuticular proteins (*Cyp4g1* and *Lcp1*) and membrane transport genes (e.g., ABC transporters; *MDR50*, *MDR65*, and *MRP1*) involved in DDT resistance for *91-R* strain (Strycharz et al. 2013). Despite previous studies pointing out *MDR50*, *MDR65*, and *MRP1* or *Cyp4g1* were more highly expressed in *91-R* strain as compared with susceptible strain *Canton-S* (Gellatly et al. 2015), those genes were not differentially transcribed in the comparison of *91-R* with *91-C*. The fact that *91-R* is 1,500-fold more resistant to DDT when compared with *Canton-S* (Strycharz et al. 2013) suggests that the possibility that *91-C* was already slightly resistant to DDT prior to the laboratory selection of *91-R* strain. This possibility is supported by previous data indicating that *91-C* strain is slightly more tolerant to DDT (7.5-fold) compared with the *Canton-S* strain (Festucci-Buselli et al. 2005).

Adaptations in the Migration of Neural Cells

Transcripts for uncoordinated-115b, *Unc-115b*, and angiopoietin-like *CG31832* are, respectively, the most constitutively up- and downregulated transcripts from the DDT resistant strain *91-R*, with both functioning to direct neuron cell movements. Specifically, *Unc-115b* is an actin-binding and LIM domain containing protein orthologous to human abLIM (Lundquist et al. 1998). It comprises part of the netrin signaling pathway that conveys guidance signals to advancing distal dendritic growth cones and determines direction of finger-like filopodia and laminopodia outgrowths into the extracellular matrix (ECM; Yang and Lundquist 2005). These nerve outgrowths involve the coordinated modulation of underlying cytoskeletal structures in response to environmental stimuli through redundant Rac GTPases MIG-2/RhoG and CED-10/Rac1(Lundquist et al. 2001), with *Unc-115b* as a downstream effector anchored to cytoskeletal F-actin (Struckhoff and Lundquist 2003). Opposing cascades of cone protrusion and retraction are initiated through interaction of cell surface receptors UNC-5 and UNC-40 (Frazzled, *fra*, or Deletion in Colorectal Cancer, DCC) with the ECM-embedded laminin-like protein, UNC-6 (Netrin-A or -B proteins; Chan et al. 1996; Leonardo et al. 1997). Coordinated movements toward UNC-6 are mediated by UNC-40 homodimers, whereas repulsive signals from UNC-6 at growth cones are mediated by interaction with UNC-5: UNC-40 heterodimers (Hong et al. 1999; MacNeil et al. 2009; Norris and Lundquist 2011). The intracellular repulsive signaling cascades mediated by UNC-5: UNC-40 involve the activation of CED-10/Rac1 and MIG-2/RhoG via the guanidine nucleotide exchange factor (GEF), UNC-73/Trio, at the UNC-40 scaffold (Forsthoefel et al. 2005; Norris et al. 2014). In contrast, the cytoplasmic domains (P1 to P3) of UNC-40 homodimers transduce attractive intracellular signals in response to UNC-6 by interactions between Rho-GTPase CDC-42 and the T-cell lymphoma Invasion and Metastasis Factor 1 (TIAM1)/*Drosophila* Still Life (sif) GEF (Demarco et al. 2012).

The *Unc-115b* CDS is within selective sweep 13 (Steele et al. 2015). The nearly 6-fold increase in transcript levels in *91-R* may be influenced by *cis*-regulatory mutations in, or flanking, TF binding sequences (fig. 3). The exact role of Unc-115b/abLIM in DDT resistance remains unclear. Regardless, functional data suggest that increased cellular concentrations of *Unc-115b* could enhance the growth, stability, or signaling to actin-based dendritic extensions. In addition to modulation of cytoskeletal dynamics, abLIMs participate in intracellular signal transduction events and impact transcription (Barrientos et al. 2007), suggesting that upregulation of *Unc-115b* may regulate transcription factor activity and be a causal factor that influences global gene expression changes predicted between *91-R* and *91-C*.

Annotations for the most highly downregulated transcript, *CG31832*, indicate functioning as a transmembrane receptor protein tyrosine kinase activator and negative regulator of apoptosis. The encoded fibrinogen C-terminal domain suggests possible roles in blood clotting and platelet (cell) aggregation as shown in its nearest ortholog, the agonistic human vascular endothelial growth factor (VEGF) family member angiopoietin 4 (ANGPT4) involved in angiogenesis (Valenzuela et al. 1999). The antagonistic *D. melanogaster* angiopoietin, *Pvf1*, inhibits apoptosis in stem cell lines (Xing et al. 2015), whereas the bovine angiopoietin ortholog, *Ang-1*, also inhibits apoptosis and promotes cell survival in

epithelial cells by activation of the Akt pathway (Papapetropoulos et al. 2000); *Ang-2* promotes apoptosis via inhibition of *Ang-1* in mouse glomeruli (Davis et al. 2007).

Angiopoietins cross-talk with Janus kinase/signal transducers and activators of transcription (JAK/STAT) and mitogen-activated protein kinase (MAPK) pathways to promote cell survival (Rychli et al. 2010). Interestingly, Netrins might regulate aspects of tumor angiogenesis (Klagsbrun and Eichmann 2005), such that analogies between guidance mechanisms in axon and capillary network formation have been made since these involve many of the same receptors and signaling ligands (Autiero et al. 2005; Freitas et al. 2008). The downregulation of the angiopoietin *CG31832* in *91-R* suggests, analogous to *Unc-115 b*, that DDT resistance in *91-R* might involve changes in neurological cell growth and maintenance. Although angiopoietin orthologs can be agonistic or antagonistic with regard to cell outgrowth and apoptosis, the downregulation of *CG31832* might be predicted to enhance axon growth or neuronal resistance to apoptosis, but additional experiments are required to investigate this.

The ECM is composed of a complex matrix of proteins and glycans involved in structural maintenance and cell signaling and is a crucial determinant of neural growth, development, and function (Broadie et al. 2011). DEGs acting within the cell migration process are observed in the upregulation of the serine proteases *Jon99Ci*, *Jon65Aii*, and *CG7542*, which function to cleave leader peptides from zymogens of MMPs. This activation of MMPs, likely by c-Jun N-terminal kinases (JNKs) or phosphatidylinositol 3 kinase (PI3K; Cheng et al. 2012), leads to the degradation of ECM components and subsequently allows for neuronal cell migration and extension of lamellipodia (Zimmermann and Dours-Zimmermann 2008), but also could modulate various growth factor signals from the ECM and thereby have a role in a range of cell processes including immune response and neuron outgrowth (Loffek et al. 2011). Additionally, MMP expression is directed by various growth factors and cytokines (Mauviel 1993) which also lead to cell responses via activation of intracellular signals from Janus protein-tyrosine kinases/transducers and activators of transcription (JAKs/STATs) classes of receptors (Ihle 1996), suggesting the coordination between ECM modulation and cell migration.

Adaptations in Neuron Cell Function

Neurotoxic effects of acute DDT exposure include characteristic twitches induced by an inhibition of the sodium channels *para* and DSC1 gate function (Rinkevich et al. 2015), the former of which is required for *Drosophila* mating behavior (Lilly et al. 1994). Furthermore, the chronic systemic effects of DDT and its metabolites are known also to impact brain development and function (Iwaniuk et al. 2006), to cause neurological defects (Grandjean and Landrigan 2014), and to influence the onset of neurological disorders (Li et al. 2015). The significantly downregulated transcript *CG3397* in *91-R* has previously been shown to be upregulated within the brain of four fly lines with *period* (*per*), *clock* (*Clk*), *timeless* (*tim*), and *cycle* (*cyc*) null mutations (Lin et al. 2002), suggesting it may possibly play a role in brain function. Alternatively, since yeast-2-hybrid evidence indicates that *CG3397* interacts with thioredoxin-like *CG11790*, which may in turn mediate redox balance in response to DDT detoxification induced oxidative stress (Li et al. 2008), but further stuides are required to further investigate the possible impacts on DDT resistance in *91-R*.

The downregulated serine protease *CG17234* and lipase *CG6277* are involved in the sensory perception of pain (Neely et al. 2010) and neurogenesis. The *CG6277* encoded phospholipase A1 (PLA1)-like domain and phosphatidylcholine 1-acylhydrolase activity (GO: 0008970) catalyze release of fatty acid groups from the 1-position of phosphatidylcholine, while RNAi-mediated knockdown causes a significant reduction in neuroblast proliferation (Neumuller et al. 2011). PLA1 has limited involvement in lysophosphatidylcholine production but is a potent regulator of phosphatidic acid levels in the testes and brain (Higgs and Glomset 1994).

Phosphatidic acid (PA) is an intermediate in the biosynthesis of phospholipids and glycolipids and is implicated in cell signaling through the binding or sequestering of proteins to membranes. For example, PA facilitates Ras activation by recruiting Son of Sevenless (SOS) to plasma membranes (Zhao et al. 2007), and similarly recruits Raf-1, which in turn induces the mitogen activated protein kinase/extracellular signal-regulating kinase (MAPK/ERK) pathway (Rizzo et al. 2000). Additionally, PA is required for activity by the homeotic sensor mammalian target of rapamycin (mTOR), which regulates progression into the cell division cycle (Foster 2013). Thus, cellular levels of PA are crucial for regulating cell survival (growth and migration) and apoptosis along with modulation of cell stress response and cytoskeletal organization (Wang et al. 2006). While the possible role of *CG6277* in DDT resistance remains undetermined, significant reduction in PLA1 activity in *91-R* may reduce PA levels in the brain, thereby attenuating or modulating the dynamics of cell growth, maintenance, and apoptosis.

Interestingly, along with *CG17234*, the knockdown of the downregulated extracellular serine protease *CG30025* has been shown to increase the sensory perception of pain from heat exposure (Neely et al. 2010). Protease-activated receptors (PARs) are G protein coupled receptors (GPCRs) expressed in tissues, including neurons, that function in the transduction of cytoplasmic signaling from extracellular proteases (Russo et al. 2009b). This occurs via specific protease-dependent N-terminal cleavages that irreversibly activate PARs (Finigan et al. 2005; Russo et al. 2009a) and thus evoke different intracellular responses, including not only the transmission of pain sensation (Bunnett 2006) but possibly also the mediation of inflammatory neuronal cell death (pyroptosis;

Li et al. 2016). These lines of evidence suggest that repression of *CG17234* and *CG30025* might be advantageous in *91-R* by reducing PAR activation and thereby hindering signal transduction of signals involved in apoptosis or the perception of pain and inflammation.

Our analysis indicates that the protein products of 8 up- and 6 downregulated transcripts in *91-R* are involved in known protein–protein interactions, where the partner proteins function in neural development or function (supplementary fig. S4, Supplementary Material online). Within these, the upregulated extracellular localized *CG15293* and downregulated endomembrane system localized reductase *CG2064* were the most highly centralized with $\geq$4 protein interactions that impact $\geq$9 neurological functions. Little is known regarding the function of these two genes, but transcription of *CG15293* is increased in response to sigma virus infection (Carpenter et al. 2009), and *CG2064* is upregulated in responses to phospholipase C2 knockdown-mediated cellular repression of ERK response to oxidative stress (Liu et al. 2007).

Additionally, physical interaction of the downregulated *CG2064* with Rab2 and Rab5 GTPases—which mediate intracellular vesicle transport (Stenmark 2009), as well as the clathrin heavy chain (Chc), Golgi vesicle transport protein, and small synaptic vesicle protein, synaptobrevin (Syb)—might be hypothesized to impact neurotransmitter release. This suggests, consonant with previous work, that *CG2064* is likely intertwined within neural function and cellular stress response pathways (Liu et al. 2007).

Changes in Cell Stress Response

Cellular reactions to stress conditions involve a delicate balance between cell survival (proliferation) and programmed death (apoptotic) pathways. Redox reactions are essential for maintaining cell homeostasis by modulating electron-transfer reactions that occur during normal metabolic processes and in response to environmental stress.

91-R exhibits constitutive upregulation of 6 cytochrome P450 monooxygenases, with only one, *Cyp4e3*, significantly downregulated. While *Drosophila Cyp6g1*, *Cyp6g2*, *Cyp6t3*, *Cyp6a2*, *Cyp6a8*, *Cyp6a19*, *Cyp6w1*, and *Cyp6a23* have been validated as DDT or imidacloprid metabolizers (Daborn et al. 2007; Morra et al. 2010; Harrop et al. 2014; Le Goff and Hilliou 2017), *Cyp4p2* and *Cyp4e3* have been found to be highly upregulated in *Drosophila* resistant to imidacloprid (Kalajdzic et al. 2012) and permethrin (Terhzaz et al. 2015). Concurring with this prior evidence, our data found a constitutive increase in *Cyp4* and *Cyp6* family transcript levels in *91-R* with the co-occurring *Cyp4e3* downregulation analogous to other insecticide-resistant insects (Yang and Liu 2011). Furthermore, DDT selection could induce elevated levels of reactive oxygen species (ROS), resulting in mitochondria-mediated apoptotic changes (Jin et al. 2014). Since P450s respond to various endogenous and exogenous compounds (Riddick 2004; Davies et al. 2006), changes in expression may enhance general stress responses, if not also remediation of specific DDT secondary metabolites.

The second most downregulated transcript, *Ser12*, physically interacts with the thioredoxin peroxidase 2, (Jafrac 2; Guruharsha et al. 2011). Thioredoxin peroxidases (Tpx) catalyze antioxidant reactions to neutralize ROS but also function in the regulation of apoptosis. The thioredoxin (Trx) redox system is based on the reversible oxidation of Trx cysteine disulfide bonds (S2) to cysteine-thiol (SH2) via concomitant reduction of equimolar equivalents of S2, which is catalyzed by the NADPH-dependent thioredoxin reductase (TrxR). Trx remediates accumulated ROS through the reduction of superoxide dismutase (sod) generated H_2O_2, often through cytosolic thioredoxin peroxidase (Tpx) or other oxidized (damaged) proteins. The Trx pathway is activated by exposure to hypoxic conditions or ROS to remediate conditions that lead to cell damage via oxidation of lipids, nucleotides, and proteins and to produce signals that increase the rate of cell growth and elevate cellular resistance to apoptosis. Furthermore, cell damage and subsequent generation of ROS act as second messengers within signal transduction cascades (Thannickal and Fanburg 2000), including the induction of apoptosis (Sarafian and Bredesen 1994). The endoplasmic-reticulum localized Jafrac2 is redistributed to the cytoplasm during apoptosis, where it interacts with the *Drosophila* inhibitor of apoptosis proteins (IAPs), DIAP1 and 2 (thread; Tenev et al. 2002). These DIAP family members possess a Baculovirus IAP Repeat (BIR) domain that acts to bind and sequester proteolytically active caspases that would otherwise initiate apoptosis in an unbound state (Crook et al. 1993). The RING finder domain of DIAP1, moreover, regulates the ubiquination, and possible endosomal degradation, of DRONC. Therefore, DIAP1 binding and inactivation of the three *Drosophila* caspases drICE (Kaiser et al. 1998), DCP-1 (Hawkins et al. 1999), and DRONC (Meier et al. 2000; Quinn et al. 2000) suppresses apoptosis. This release of Jafrac2, however, is contingent upon N-terminal cleavage exposing an IAP-binding motif (IBM) to allow subsequent competitive displacement of the active form of the caspase DRONC from DIAP1. Based upon this observed colocalization, we propose that the serine protease *Ser12* may constitute an endoplasmic reticulum protease able to N-terminal cleave Jafrac2, which upon subsequent downregulation in *91-R* may hinder transport of Jafrac2 to the cytoplasm, thereby suppressing the onset or progression of apoptotic events.

Serine proteases are a diverse family of proteolytic enzymes involved in a wide array of extracellular processes, including digestion, immune response, degradation of extracellular matrix components, and inflammation, along with intracellular protein cycling, apoptosis, and mediation of signal transduction events (Weiss 1989; Puente et al. 2005; Ramachandran and Hollenberg 2009). Four serine-like proteases, *Jon99Fii*, *CG4927*, *CG17234*, *CG30025*, and *Ser12* are downregulated

in *91-R*. Previous research showed that *Ser12* mutation can alter epithelial wound healing capacity (Campos et al. 2010) and is analogous to GO annotations and RNAi knockdown for *PPO 1* and the glycoside hydrolase/chitinase II and imaginal disc growth factor 1, *Idfg1* (Pesch et al. 2016). Systemic wound response is orchestrated by the serine protease-mediated conversion of PPO to phenoloxidase (PO) (Bidla et al. 2009), which in turn converts monophenols to o-quinones during melanin nodule and scab formation (Galko and Krasnow 2004), with the hemolymph hayan protease (*CG6361*) cleaving PPO to the activated PO (Nam et al. 2012). Additionally, c-JNK is activated in response to cell wounding (Rämet et al. 2002) and triggers cell migration during wound closure (Lesch et al. 2010).

Since PO-catalyzed melanization reactions result in the production of ROS (Nappi and Vass 1993), an integrated system of cellular response has been described. Specifically, serine proteases were shown to trigger JNK-dependent activation of redox pathways in *D. melanogaster* (Nam et al. 2012), which may serve to protect cells from oxidative damage during wound healing. Results from this study disclose a constitutive downregulation of *PPO1* and *2*, as well as an upregulation of serine protease inhibitors, serpin *Spn43Aa* and the Kunitz trypsin-inhibitor domain-containing, *sfp24Ba*, in *91-R*. These suggest that adaptations resulting in decreased endogenous ROS production in response to (xenobiotic-induce) cell damage may counterbalance the excess produced when detoxifying high levels of xenobiotics like DDT. Since hemolymph ROS are systemic, organism-wide upregulation of these protective redox mechanisms may be selectively advantageous.

Three serine-like proteases, *CG7542*, *Jon99Ci*, and *Jon65Aii*, are upregulated in *91-R*, with the latter two involved in Toll-signaling. The *Drosophila* Toll pathway helps to modulate cellular immune response as well as several developmental events (Valanne et al. 2011) and is regulated via serpin family protease inhibitors that also directly control melanization via phenol oxidases (Ligoxygakis et al. 2002). Products from the upregulated *CG43055* and *Lectin-galC1* (located in selective sweep 5) transcripts have C-lectin domains that define extracellular, carbohydrate-binding, Ca^{2+}-dependent cell surface adhesion proteins involved in agglutination and hemocyte-mediation mechanism during bacterial infection response (Tanji et al. 2006). C-type lectins initiate immune response via a diverse set of signaling pathways including through *PPO1* and *PPO2* (Geijtenbeek and Gringhuis 2009).

Conclusions

The regulation of gene expression is an important mechanism by which organisms respond and adapt to their environment (Carroll 2000). In this study, we identified a total of 69 constitutive DEGs in *91-R* as compared with *91-C* strains, and wherein identified DEGs associated with neural cell development, signal transduction, and gene regulatory cascades. When comparing the current functional data to prior structure mutation data, only 6 out of 69 DEGs were physically linked to 1 of the 13 different genome regions showing evidence of strong directional selection between strains (selective sweeps; Steele et al. 2015). Therefore, it remains difficult to make concrete associations between structural and functional changes in *91-R* in relation to the evolution of DDT resistance. For example, even though mutations within *91-R* were predicted in the CRE-BP1 and flanking the BEAF-32 consensus TF binding sequence upstream of the most highly upregulated transcript, *Unc-115b*, the fact that mutations remaining segregating remains difficult to resolve for subsequent associations with DDT resistance when dominance of the alleles or other factors influencing expression in the genome architecture of *91-R* are unknown. Furthermore, in spite of evidence that selective sweeps have likely occurred in response to directional selection of DDT exposure in *91-R*, the specious associations with ancestral neutral mutations embedded within these sweeps, as well as across the entire genome, that have been impacted by random genetic drift since strains with a common genetic background ~60 years ago cannot be ruled out. Regardless, the majority of environment-dependent changes in gene expression are predicted to be caused by trans- and cis-acting regulatory mutations (Grundberg et al. 2011; Fear et al. 2016), suggesting that regulatory complexity for gene expression may be important to modulating adaptive divergence. Further studies are undoubtedly required in order to directly correlate structural mutations with complex changes in systemic regulation of gene expression.

Given the above caveats, this current study does provide novel evidence that alteration of neurological function or neurogenesis may be associated with DDT resistance in *91-R*. Specifically, this is shown for the most highly upregulated transcript in *91-R*, the actin-binding *Unc-115b*, that functions in axon guidance and maintenance, and the most downregulated transcript, the angiopoietin-like *CG31832*, which has a putative vascular and neural guidance function. One might suggest that the most dramatic changes in constitutive gene expression, both impacting the regulation of neural cell migration or maintenance (survival/resistance to apoptosis), may not be coincidental, and possibly be contributing factors in the adaption of *91-R* to high DDT exposure levels. Furthermore, the second most downregulated transcript, *Ser12*, comprises a proteolytic putative activator of the thioredoxin 2, *Jafrac2*. This reduced expression of *Ser12* might be hypothesized to reduce to proteolytic cleavage of *Jafrac2* and subsequently inhibit cell progression into apoptosis. While the current study provides enticing insights into the evolution of DDT resistance in *91-R*, additional functional evidence is required to establish causation with respect to axon growth and cellular resistance to apoptosis pathways. Additional experiments utilizing analysis of reselected recombinant inbred lines (RILs), and reverse

genetics will likely be required to identify the causal basis of DDT resistance in *91-R*, thus results here must be interpreted with caution.

Supplementary Material

Supplementary data are available at *Genome Biology and Evolution* online.

Acknowledgments

The authors declare that they have no competing interests relevant to the work and data reported here.

Author Contributions

K.M.S. performed most of the experiments with the help of W.S. and B.S.C. K.M.S. and B.S.C. analyzed high-throughput sequencing data. K.M.S. and B.S.C. wrote the manuscript assisted by B.R.P. and J.M.C. All authors read and approved the final manuscript.

Literature Cited

Afschar S, et al. 2016. Nuclear hormone receptor DHR96 mediates the resistance to xenobiotics but not the increased lifespan of insulin-mutant *Drosophila*. Proc Natl Acad Sci U S A. 113(5):1321–1326.

Allison DB, Cui X, Page GP, Sabripour M. 2006. Microarray data analysis: from disarray to consolidation and consensus. Nat Rev Genet 7(1):55–65.

Autiero M, De Smet F, Claes F, Carmeliet P. 2005. Role of neural guidance signals in blood vessel navigation. Cardiovasc Res 65:629–638.

Barrientos T, et al. 2007. Two novel members of the ABLIM protein family, ABLIM-2 and-3, associate with STARS and directly bind F-actin. J Biol Chem 282(11):8393–8403.

Benjamini Y, Hochberg Y. 1995. Controlling the false discovery rate: a practical and powerful approach to multiple testing. J R Stat Soc Series B Stat Methodol 57:289–300.

Bidla G, Hauling T, Dushay MS, Theopold U. 2009. Activation of insect phenoloxidase after injury: endogenous versus foreign elicitors. J Innate Immun 1(4):301–308.

Brandt A, et al. 2002. Differential expression and induction of two *Drosophila* cytochrome P450 genes near the Rst (2) DDT locus. Insect Mol Biol 11(4):337–341.

Broadie K, Baumgartner S, Prokop A. 2011. Extracellular matrix and its receptors in *Drosophila* neural development. Dev Neurobiol 71(11):1102–1130.

Bunnett NW. 2006. Protease-activated receptors: how proteases signal to cells to cause inflammation and pain. Semin Thromb Hemost 32(S 1):39–48.

Campos I, Geiger JA, Santos AC, Carlos V, Jacinto A. 2010. Genetic screen in *Drosophila melanogaster* uncovers a novel set of genes required for embryonic epithelial repair. Genetics 184(1):129–140.

Carpenter J, et al. 2009. The transcriptional response of *Drosophila melanogaster* to infection with the sigma virus (*Rhabdoviridae*). PLoS One 4(8):e6838.

Carroll SB. 2000. Endless forms: the evolution of gene regulation and morphological diversity. Cell 101(6):577–580.

Chan S-Y, et al. 1996. UNC-40, a *C. elegans* homolog of DCC (Deleted in Colorectal Cancer), is required in motile cells responding to UNC-6 netrin cues. Cell 87(2):187–195.

Cheng CY, Hsieh HL, Hsiao LD, Yang CM. 2012. PI3-K/Akt/JNK/NF-κB is essential for MMP-9 expression and outgrowth in human limbal epithelial cells on intact amniotic membrane. Stem Cell Res 9(1):9–23.

Crook NE, Clem RJ, Miller LK. 1993. An apoptosis-inhibiting baculovirus gene with a zinc finger-like motif. J Virol 67(4):2168–2174.

Daborn PJ, et al. 2007. Evaluating the insecticide resistance potential of eight *Drosophila melanogaster* cytochrome P450 genes by transgenic over-expression. Insect Biochem Mol Biol 37(5):512–519.

Davies L, et al. 2006. Expression and down-regulation of cytochrome P450 genes of the CYP4 family by ecdysteroid agonists in *Spodoptera littoralis* and *Drosophila melanogaster*. Insect Biochem Mol Biol 36(10):801–807.

Davis B, et al. 2007. Podocyte-specific expression of angiopoietin-2 causes proteinuria and apoptosis of glomerular endothelia. J Am Soc Nephrol 18(8):2320–2329.

Demarco RS, Struckhoff EC, Lundquist EA. 2012. The Rac GTP exchange factor TIAM-1 acts with CDC-42 and the guidance receptor UNC-40/DCC in neuronal protrusion and axon guidance. PLoS Genet 8(4):e1002665.

Dos Santos G, et al. 2015. FlyBase: introduction of the *Drosophila melanogaster* Release 6 reference genome assembly and large-scale migration of genome annotations. Nucleic Acids Res 43(Database issue):D690–D697.

Fear JM, et al. 2016. Buffering of genetic regulatory networks in *Drosophila melanogaster*. Genetics 203(3):1177–1190.

Festucci-Buselli RA, et al. 2005. Expression of Cyp6g1 and Cyp12d1 in DDT resistant and susceptible strains of *Drosophila melanogaster*. Insect Mol Biol 14(1):69–77.

Ffrench-Constant RH. 2013. The molecular genetics of insecticide resistance. Genetics 194(4):807.

Ffrench-Constant RH, Daborn PJ, Le Goff G. 2004. The genetics and genomics of insecticide resistance. Trends Genet 20(3):163–170.

Ffrench-Constant RH, Rocheleau TA, Steichen JC, Chalmers AE. 1993. A point mutation in a *Drosophila* GABA receptor confers insecticide resistance. Nature 363(6428):449–451.

Finigan JH, et al. 2005. Activated protein C mediates novel lung endothelial barrier enhancement role of sphingosine 1-phosphate receptor transactivation. J Biol Chem 280(17):17286–17293.

Forsthoefel DJ, Liebl EC, Kolodziej PA, Seeger MA. 2005. The abelson tyrosine kinase, the trio GEF and enabled interact with the netrin receptor frazzled in *Drosophila*. Development 132(8):1983–1994.

Foster DA. 2013. Phosphatidic acid and lipid-sensing by mTOR. Trends Endocrinol Metab 24(6):272–278.

Freitas C, Larrivée B, Eichmann A. 2008. Netrins and UNC5 receptors in angiogenesis. Angiogenesis 11(1):23–29.

Galbraith C, Skalak R, Chien S. 1998. Shear stress induces spatial reorganization of the endothelial cell cytoskeleton. Cytoskeleton 40(4):317–330.

Galko MJ, Krasnow MA. 2004. Cellular and genetic analysis of wound healing in *Drosophila* larvae. PLoS Biol 2(8):e239.

Gehart H, Kumpf S, Ittner A, Ricci R. 2010. MAPK signalling in cellular metabolism: stress or wellness? EMBO Reports 11(11):834–840.

Geijtenbeek TB, Gringhuis SI. 2009. Signalling through C-type lectin receptors: shaping immune responses. Nat Rev Immunol 9(7):465–479.

Gellatly KJ, et al. 2015. RNAi validation of resistance genes and their interactions in the highly DDT-resistant 91-R strain of *Drosophila melanogaster*. Pestic Biochem Physiol 121:107–115.

Grandjean P, Landrigan PJ. 2014. Neurobehavioural effects of developmental toxicity. Lancet Neurol. 13(3):330–338.

Grundberg E, et al. 2011. Global analysis of the impact of environmental perturbation on *cis*-regulation of gene expression. PLoS Genet 7(1):e1001279.
Guertin M, Petesch S, Zobeck K, Min I, Lis J. 2010. *Drosophila* heat shock system as a general model to investigate transcriptional regulation. Cold Spring Harb Symp Quant Biol 75:1–9.
Guruharsha K, et al. 2011. A protein complex network of *Drosophila melanogaster*. Cell 147(3):690–703.
Harrop TW, et al. 2014. Evolutionary changes in gene expression, coding sequence and copy-number at the *Cyp6g1* locus contribute to resistance to multiple insecticides in *Drosophila*. PLoS One 9:e84879.[CVOCROSSCVO]
Hawkins CJ, Wang SL, Hay BA. 1999. A cloning method to identify caspases and their regulators in yeast: identification of *Drosophila* IAP1 as an inhibitor of the *Drosophila* caspase DCP-1. Proc Natl Acad Sci U S A. 96(6):2885–2890.
Higgs HN, Glomset JA. 1994. Identification of a phosphatidic acid-preferring phospholipase A1 from bovine brain and testis. Proc Natl Acad Sci U S A. 91(20):9574–9578.
Hong K, et al. 1999. A ligand-gated association between cytoplasmic domains of UNC5 and DCC family receptors converts netrin-induced growth cone attraction to repulsion. Cell 97(7):927–941.
Ihle JN. 1996. STATs: signal transducers and activators of transcription. Cell 84(3):331–334.
Iwaniuk AN, et al. 2006. The effects of environmental exposure to DDT on the brain of a songbird: changes in structures associated with mating and song. Behav Brain Res 173(1):1–10.
Jin X, et al. 2014. Protective efficacy of vitamins C and E on p, p'-DDT-induced cytotoxicity via the ROS-mediated mitochondrial pathway and NF-kappaB/FasL pathway. PLoS One 9(12):e113257.
Kaiser WJ, Vucic D, Miller LK. 1998. The *Drosophila* inhibitor of apoptosis D-IAP1 suppresses cell death induced by the caspase drICE. FEBS Lett 440(1–2):243–248.
Kalajdzic P, et al. 2012. Use of mutagenesis, genetic mapping and next generation transcriptomics to investigate insecticide resistance mechanisms. PLoS One 7(6):e40296.
Klagsbrun M, Eichmann A. 2005. A role for axon guidance receptors and ligands in blood vessel development and tumor angiogenesis. Cytokine Growth Factor Rev 16(4–5):535–548.
Le Goff G, Hilliou F. 2017. Resistance evolution in *Drosophila*: the case of CYP6G1. Pest Manag Sci. 73(3):493–499.
Leonardo ED, et al. 1997. Vertebrate homologues of *C. elegans* UNC-5 are candidate netrin receptors. Nature 386(6627):833–838.
Lesch C, Jo J, Wu Y, Fish GS, Galko MJ. 2010. A targeted UAS-RNAi screen in *Drosophila* larvae identifies wound closure genes regulating distinct cellular processes. Genetics 186(3):943–957.
Li G, et al. 2015. Common pesticide, dichlorodiphenyltrichloroethane (DDT), increases Amyloid-β levels by impairing the function of ABCA1 and IDE: implication for Alzheimer's. Disease. J Alzheimers Dis 46(1):109–122.
Li X, Tang K, Xie B, Li S, Rozanski GJ. 2008. Regulation of Kv4 channel expression in failing rat heart by the thioredoxin system. Am J Physiol Heart Circ Physiol 295(1):H416–H424.
Li Y, et al. 2016. Interference with protease-activated receptor 1 alleviates neuronal cell death induced by lipopolysaccharide-stimulated microglial cells through the PI3K/Akt pathway. Sci Rep 6:38247.
Ligoxygakis P, et al. 2002. A serpin mutant links Toll activation to melanization in the host defence of *Drosophila*. EMBO 21(23):6330–6337.
Lilly M, Kreber R, Ganetzky B, Carlson J. 1994. Evidence that the *Drosophila* olfactory mutant smellblind defines a novel class of sodium channel mutation. Genetics 136(3):1087–1096.
Lin Y, et al. 2002. Influence of the period-dependent circadian clock on diurnal, circadian, and aperiodic gene expression in *Drosophila melanogaster*. Proc Natl Acad Sci U S A. 99(14):9562–9567.
Liu W, Silverstein AM, Shu H, Martinez B, Mumby MC. 2007. A functional genomics analysis of the B56 isoforms of *Drosophila* protein phosphatase 2A. Mol Cell Proteomics 6(2):319–332.
Livak KJ, Schmittgen TD. 2001. Analysis of relative gene expression data using real-time quantitative PCR and the $2^{-\Delta\Delta CT}$ method. Methods 25(4):402–408.
Loffek S, Schilling O, Franzke CW. 2011. Series "matrix metalloproteinases in lung health and disease": biological role of matrix metalloproteinases: a critical balance. Eur Respir J 38(1):191–208.
Lundquist EA, Herman RK, Shaw JE, Bargmann CI. 1998. UNC-115, a conserved protein with predicted LIM and actin-binding domains, mediates axon guidance in *C. elegans*. Neuron 21(2):385–392.
Lundquist EA, Reddien PW, Hartwieg E, Horvitz HR, Bargmann CI. 2001. Three *C. elegans* Rac proteins and several alternative Rac regulators control axon guidance, cell migration and apoptotic cell phagocytosis. Development 128(22):4475–4488.
MacNeil LT, Hardy WR, Pawson T, Wrana JL, Culotti JG. 2009. UNC-129 regulates the balance between UNC-40 dependent and independent UNC-5 signaling pathways. Nat Neurosci 12(2):150–155.
Mallet J. 1989. The evolution of insecticide resistance: have the insects won? Trends Ecol Evol 4(11):336–340.
Martin RL, et al. 2000. Point mutations in domain III of a *Drosophila* neuronal Na channel confer resistance to allethrin. Insect Biochem Mol Biol. 30(11):1051–1059.
Mauviel A. 1993. Cytokine regulation of metalloproteinase gene expression. J Cell Biochem 53(4):288–295.
Meier P, Silke J, Leevers SJ, Evan GI. 2000. The *Drosophila* caspase DRONC is regulated by DIAP1. Embo J 19(4):598–611.
Merrell DJ. 1960. Heterosis in DDT resistant and susceptible populations of *Drosophila melanogaster*. Genetics 45(5):573–581.
Merrell DJ. 1965. Lethal frequency and allelism in DDT resistant populations and their controls. Am. Nat. 99(908):411–417.
Merrell DJ, Underhill JC. 1956. Selection for DDT resistance in inbred, laboratory and wild stocks of *Drosophila melanogaster*. J Econ Entomol 49(3):300–306.
Misra JR, Lam G, Thummel CS. 2013. Constitutive activation of the Nrf2/Keap1 pathway in insecticide-resistant strains of *Drosophila*. Insect Biochem Mol Biol 43(12):1116–1124.
Morra R, Kuruganti S, Lam V, Lucchesi J, Ganguly R. 2010. Functional analysis of the cis-acting elements responsible for the induction of the Cyp6a8 and Cyp6g1 genes of *Drosophila melanogaster* by DDT, phenobarbital and caffeine. Insect Mol Biol 19(1):121–130.
Najarro MA, et al. 2015. Identifying loci contributing to natural variation in xenobiotic resistance in *Drosophila*. PLoS Genet 11(11): e1005663.
Nam HJ, Jang IH, You H, Lee KA, Lee WJ. 2012. Genetic evidence of a redox-dependent systemic wound response via Hayan protease-phenoloxidase system in *Drosophila*. Embo J 31(5):1253–1265.
Nappi A, Vass E. 1993. Melanogenesis and the generation of cytotoxic molecules during insect cellular immune reactions. Pigment Cell Melanoma Res 6(3):117–126.
Neely GG, et al. 2010. A genome-wide *Drosophila* screen for heat nociception identifies $\alpha 2\delta 3$ as an evolutionarily conserved pain gene. Cell 143(4):628–638.
Neumuller RA, et al. 2011. Genome-wide analysis of self-renewal in *Drosophila* neural stem cells by transgenic RNAi. Cell Stem Cell 8(5):580–593.
Norris AD, Lundquist EA. 2011. UNC-6/netrin and its receptors UNC-5 and UNC-40/DCC modulate growth cone protrusion in vivo in *C. elegans*. Development 138(20):4433–4442.
Norris AD, Sundararajan L, Morgan DE, Roberts ZJ, Lundquist EA. 2014. The UNC-6/Netrin receptors UNC-40/DCC and UNC-5 inhibit growth cone filopodial protrusion via UNC-73/Trio, Rac-like GTPases and UNC-33/CRMP. Development 141(22):4395–4405.

Papapetropoulos A, et al. 2000. Angiopoietin-1 inhibits endothelial cell apoptosis via the Akt/survivin pathway. J Biol Chem 275(13):9102–9105.
Pedra J, McIntyre L, Scharf M, Pittendrigh BR. 2004. Genome-wide transcription profile of field-and laboratory-selected dichlorodiphenyltrichloroethane (DDT)-resistant *Drosophila*. Proc Natl Acad Sci U S A. 101(18):7034–7039.
Pesch YY, Riedel D, Patil KR, Loch G, Behr M. 2016. Chitinases and Imaginal disc growth factors organize the extracellular matrix formation at barrier tissues in insects. Sci Rep 6:18340.
Pittendrigh BR, Reenan R, Ffrench-Constant RH, Ganetzky B. 1997. Point mutations in the *Drosophila* sodium channel gene *para* associated with resistance to DDT and pyrethroid insecticides. Mol Gen Genet 256(6):602–610.
Ponton F, Chapuis M-P, Pernice M, Sword GA, Simpson SJ. 2011. Evaluation of potential reference genes for reverse transcription-qPCR studies of physiological responses in *Drosophila melanogaster*. J Insect Physiol 57(6):840–850.
Puente XS, Sánchez LM, Gutiérrez-Fernández A, Velasco G, López-Otín C. 2005. A genomic view of the complexity of mammalian proteolytic systems. Biochem Soc Trans 33(2):331–334.
Qiu X, et al. 2013. Genome-wide analysis of genes associated with moderate and high DDT resistance in *Drosophila melanogaster*. Pest Manag Sci 69(8):930–937.
Quinn LM, et al. 2000. An essential role for the caspase dronc in developmentally programmed cell death in *Drosophila*. J Biol Chem 275(51):40416–40424.
Ramachandran R, Hollenberg M. 2009. Proteinases and signalling: pathophysiological and therapeutic implications via PARs and more. Br J Pharmacol 153(S1):S263–S282.
Rämet M, Lanot R, Zachary D, Manfruelli P. 2002. JNK signaling pathway is required for efficient wound healing in *Drosophila*. Dev Biol 241(1):145–156.
Ranson H, Lissenden N. 2016. Insecticide resistance in African *Anopheles* mosquitoes: a worsening situation that needs urgent action to maintain malaria control. Trends Parasitol 32(3):187–196.
Riddick DS. 2004. Transcriptional suppression of cytochrome P450 genes by endogenous and exogenous chemicals. Drug Metab Dispos 32(4):367–375.
Rinkevich FD, et al. 2015. Distinct roles of the DmNa v and DSC1 channels in the action of DDT and pyrethroids. Neurotoxicology 47:99–106.
Rizzo MA, Shome K, Watkins SC, Romero G. 2000. The recruitment of Raf-1 to membranes is mediated by direct interaction with phosphatidic acid and is independent of association with Ras. J Biol Chem 275(31):23911–23918.
Robinson MD, McCarthy DJ, Smyth GK. 2010. EdgeR: a Bioconductor package for differential expression analysis of digital gene expression data. Bioinformatics 26(1):139–140.
Robinson MD, Smyth GK. 2007. Moderated statistical tests for assessing differences in tag abundance. Bioinformatics 23(21):2881–2887.
Robinson MD, Smyth GK. 2008. Small-sample estimation of negative binomial dispersion, with applications to SAGE data. Biostatistics 9(2):321–332.
Russo A, Soh UJ, Paing MM, Arora P, Trejo J. 2009a. Caveolae are required for protease-selective signaling by protease-activated receptor–1. Proc Natl Acad Sci U S A. 106(15):6393–6397.
Russo A, Soh UJ, Trejo J. 2009b. Proteases display biased agonism at protease-activated receptors: location matters! Mol Interv 9:87–96.
Rychli K, et al. 2010. The inflammatory mediator oncostatin M induces angiopoietin 2 expression in endothelial cells *in vitro* and *in vivo*. J Thromb Haemost 8(3):596–604.
Sarafian TA, Bredesen DE. 1994. Invited commentary is apoptosis mediated by reactive oxygen species? Free Radic Res 21(1):1–8.
Seong KM, Sun W, Clark JM, Pittendrigh BR. 2016. Splice form variant and amino acid changes in MDR49 confers DDT resistance in transgenic *Drosophila*. Sci Rep 6:23355.
Shannon P, et al. 2003. Cytoscape: a software environment for integrated models of biomolecular interaction networks. Genome Res 13(11): 2498–2504.
Shaposhnikov M, Proshkina E, Shilova L, Zhavoronkov A, Moskalev A. 2015. Lifespan and stress resistance in *Drosophila* with overexpressed DNA repair genes. Sci Rep 5:15299.
Slack C, et al. 2010. Regulation of lifespan, metabolism, and stress responses by the *Drosophila* SH2B protein, Lnk. PLoS Genet 6(3): e1000881.
Slack C, Giannakou ME, Foley A, Goss M, Partridge L. 2011. dFOXO-independent effects of reduced insulin-like signaling in *Drosophila*. Aging Cell 10(5):735–748.
Spriggs KA, Bushell M, Willis AE. 2010. Translational regulation of gene expression during conditions of cell stress. Mol Cell 40(2): 228–237.
Steele LD, et al. 2014. Genome-wide sequencing and an open reading frame analysis of dichlorodiphenyltrichloroethane (DDT) susceptible (*91-C*) and resistant (*91-R*) *Drosophila melanogaster* laboratory populations. PLoS One 9(6):e98584.
Steele LD, et al. 2015. Selective sweep analysis in the genomes of the *91-R* and *91-C Drosophila melanogaster* strains reveals few of the 'usual suspects' in dichlorodiphenyltrichloroethane (DDT) resistance. PLoS One 10(3):e0123066.
Stenmark H. 2009. Rab GTPases as coordinators of vesicle traffic. Nat Rev Mol Cell Biol 10(8):513–525.
Struckhoff EC, Lundquist EA. 2003. The actin-binding protein UNC-115 is an effector of Rac signaling during axon pathfinding in *C. elegans*. Development 130(4):693–704.
Strycharz JP, et al. 2013. Resistance in the highly DDT-resistant *91-R* strain of *Drosophila melanogaster* involves decreased penetration, increased metabolism, and direct excretion. Pestic Biochem Physiol 107(2): 207–217.
Sun W, et al. 2015. A glycine insertion in the estrogen-related receptor (ERR) is associated with enhanced expression of three cytochrome P450 genes in transgenic *Drosophila melanogaster*. PLoS One 10(3): e0118779.
Szklarczyk D, et al. 2015. STRING v10: protein–protein interaction networks, integrated over the tree of life. Nucleic Acids Res 43(D1): 447–452.
Tanji T, Ohashi-Kobayashi A, Natori S. 2006. Participation of a galactose-specific C-type lectin in *Drosophila* immunity. Biochem J 396(1): 127–138.
Tenev T, Zachariou A, Wilson R, Paul A, Meier P. 2002. Jafrac2 is an IAP antagonist that promotes cell death by liberating Dronc from DIAP1. Embo J 21(19):5118–5129.
Terhzaz S, et al. 2015. A novel role of *Drosophila* cytochrome *P450-4e3* in permethrin insecticide tolerance. Insect Biochem Mol Biol 67: 38–46.
Thannickal VJ, Fanburg BL. 2000. Reactive oxygen species in cell signaling. Am J Physiol Lung Cell Mol Physiol 279(6):L1005–L1028.
Tower J. 2011. Heat shock proteins and *Drosophila* aging. Exp Gerontol 46(5):355–362.
Tzima E, et al. 2002. Activation of Rac1 by shear stress in endothelial cells mediates both cytoskeletal reorganization and effects on gene expression. Embo J 21(24):6791–6800.
Valanne S, Wang J-H, Rämet M. 2011. The *Drosophila* toll signaling pathway. Journal Immunol. 186(2):649–656.
Valenzuela DM, et al. 1999. Angiopoietins 3 and 4: diverging gene counterparts in mice and humans. Proc Natl Acad Sci U S A. 96(5):1904–1909.

Wang MC, Bohmann D, Jasper H. 2003. JNK signaling confers tolerance to oxidative stress and extends lifespan in *Drosophila*. Dev Cell 5(5):811–816.

Wang X, Devaiah SP, Zhang W, Welti R. 2006. Signaling functions of phosphatidic acid. Prog Lipid Res. 45(3):250–278.

Weiss SJ. 1989. Tissue destruction by neutrophils. N Engl J Med 320(6):365–376.

Xing Y, Su TT, Ruohola-Baker H. 2015. Tie-mediated signal from apoptotic cells protects stem cells in *Drosophila melanogaster*. Nat Commun 6:7058.

Yang T, Liu N. 2011. Genome analysis of cytochrome P450s and their expression profiles in insecticide resistant mosquitoes, *Culex quinquefasciatus*. PLoS One 6(12):e29418.

Yang Y, Lundquist EA. 2005. The actin-binding protein UNC-115/abLIM controls formation of lamellipodia and filopodia and neuronal morphogenesis in *Caenorhabditis elegans*. Mol Cell Biol 25(12):5158–5170.

Zhao C, Du G, Skowronek K, Frohman MA, Bar-Sagi D. 2007. Phospholipase D2-generated phosphatidic acid couples EGFR stimulation to Ras activation by Sos. Nat Cell Biol 9(6):707–712.

Zimmermann DR, Dours-Zimmermann MT. 2008. Extracellular matrix of the central nervous system: from neglect to challenge. Histochem Cell Biol 130(4):635–653.

Associate editor: Yoshihito Niimura